

## Engineered Residual Stress to Mitigate Stress Corrosion Cracking of Stainless Steel Weldments

Jeremy E. Scheel, N. Jayaraman, Douglas J. Hornbach  
Lambda Technologies  
5521 Fair Lane  
Cincinnati, OH, 45227-3401  
USA

### ABSTRACT

Stress corrosion cracking (SCC) is the result of the combined influence of tensile stress and a corrosive environment on a susceptible material. Austenitic stainless steels including types 304L and 316L are susceptible alloys commonly used in nuclear weldments. An engineered residual stress field can be introduced into the surface of components that can reliably produce thermo-mechanically stable, deep compressive residual stresses to mitigate SCC. The stability of the residual stresses is dependant on the amount of cold working produced during surface enhancement processing.

Three different symmetrical geometries of weld mockups were processed using low plasticity burnishing (LPB) to produce the desired compressive residual stress field on half of each specimen. SCC testing in boiling  $MgCl_2$  was performed to compare the LPB treated and un-treated 304L and 316L stainless steel weldments. X-ray diffraction residual stress analyses were used to document the respective residual stress fields and percent cold working of each condition. Testing was performed to quantify the thermo-mechanical stability of the residual stresses. The un-treated weldments suffered severe SCC damage due to the residual tension from the welding operation. The results show conclusively that LPB completely mitigated SCC in the tested weldments and provided thermo-mechanically stable, deep residual compression.

### KEYWORDS:

Stress Corrosion Cracking, Low Plasticity Burnishing, Residual Stress, Weldments, Nuclear Reactor, Stainless Steel.

## INTRODUCTION

SCC is one of the most serious metallurgical problems facing many industries today. Studies have revealed that all grades and conditions of austenitic stainless steels and Ni based alloys are in fact susceptible to SCC given the right environment and conditions and subject to either applied or residual tensile stress.<sup>1</sup> Material degradation problems due to SCC have cost the U.S. nuclear industry over 10 billion dollars in the last thirty years.<sup>2</sup> SCC is a direct cause of increased inspection requirements and extensive component repairs and/or replacements. A cost effective means of mitigating SCC would greatly reduce operational and maintenance costs.

A combination of a susceptible material, corrosive environment and tensile stress over a threshold limit will result in SCC. Welding, machining fit up and other fabrication processes can produce high tensile residual stresses and cold working in the surface and near surface material of critical components.<sup>3,4</sup> Furthermore, SCC can occur at stresses well within the range of typical design stress thus presenting an obvious concern.<sup>5</sup> The conventional approach to mitigate the problem has been to develop new alloys, which are more resistant to SCC. A more cost effective method is to induce a compressive residual stress into the critical regions of the weldment. Conventional surface enhancement techniques such as shot peening (SP), needle peening and cavitation peening are currently being used in the nuclear industry to mitigate or impede SCC by inducing compressive residual stresses into the surface material.<sup>6,7</sup>

These conventional forms of shot peening and other similar surface treatments are beneficial due to the compressive residual stresses generated at the surface of the material being processed. However, the depth of compression achieved by these methods is typically shallow. Furthermore, these operations cause a considerable amount of cold working that can exceed 50%. High levels of cold work further increase the susceptibility for SCC initiation and produce a thermo-mechanically unstable residual stress state. Stability of the residual compression is particularly significant in the high temperature applications seen in BWR or PWR systems as well as in the event of excursions in stress exceeding the proportional limit of the alloy.

Advanced surface enhancement methods including laser peening (LP)<sup>8</sup> and LPB have been shown to more effectively mitigate SCC by producing a much deeper layer of stable residual compression than conventional peening technologies. The ability to produce a deep layer of thermo-mechanically stable compression is paramount in preventing SCC. LPB is a unique, component specific process, which imparts a deep layer of stable residual compressive stress with characteristic controlled low cold working on the order of 3-5%. The low cold work of LPB provides for a stable, compressive stress field under thermal and mechanical cycling.

LPB has been successfully applied to mitigate SCC in 300M HSLA steel (UNS# K44220) used in aircraft landing gear<sup>9,10</sup>; AA7076-T6 (UNS# A97076) propeller taper bores, and closure lid welds on Alloy 22 (UNS# N06022) nuclear waste containment canisters. By engineering a custom residual stress distribution into metals it is possible to mitigate or entirely prevent SCC initiation.<sup>11,12</sup>

## EXPERIMENTAL PROCEDURE

### Material and Processing

Specimens of 304L (UNS# S30403) and 316L (UNS# S31603) SS were manufactured. Three symmetrical geometries were used for testing: Square plates with a single circular TIG weld centered on the specimen of nominal dimensions 4 x 4 x 0.5 in. (102 x 102 x 13 mm), pipe weld specimens of schedule 40 pipe welded together with an outside diameter of 3.5 in. (89 mm), and rectangular welded v groove specimens of nominal dimensions of 1 x 6 x 12 in. (25 x 152 x 305 mm). Chemical composition and mechanical properties for the materials used are shown in Table 1. Plate material was processed per ASME SA240; ER308 (UNS# S30800) weld material was deposited longitudinally along V grooves on both sides of each plate and then ground flush to the parent metal. The final surface of the parent metal was ground prior to LPB processing.

LPB processing was performed on a 4-axis CNC mill. The square and rectangular welded plate specimens were LPB processed along half of each specimen using single point LPB tooling as shown in Figure 1. Figures 2 and 3 show both geometries after LPB processing. The sections of schedule 40 pipe were welded together using a typical butt weld then LPB processed, using a double ball caliper tool, on both the inside and outside diameters of the welded pipes. A finished pipe weld specimen is shown in Figure 4.

**TABLE 1**

ELEMENTAL COMPOSITION		
Element	304L SS (Cert. # 330580 05)	316L SS (Cert. # 422820 06)
C	0.064	0.0193
Co	-	0.1875
Cr	18.036	16.7437
Cu	0.353	0.3842
Mn	1.953	1.4095
Mo	0.353	2.1650
N	0.035	0.0413
Ni	8.045	10.2527
P	0.030	0.0335
S	<0.001	0.0002
Si	0.301	0.3372
Fe	Remainder	Remainder

MECHANICAL PROPERTIES					
Material	UTS (ksi)	0.2% YS (ksi)	% Elong 2 in.	Hardness (RB)	
304 SS	91.74	46.03	62.00	85.50	
316 SS	89.97	45.87	65.00	73.00	



Figure 1: LPB Processing of specimens

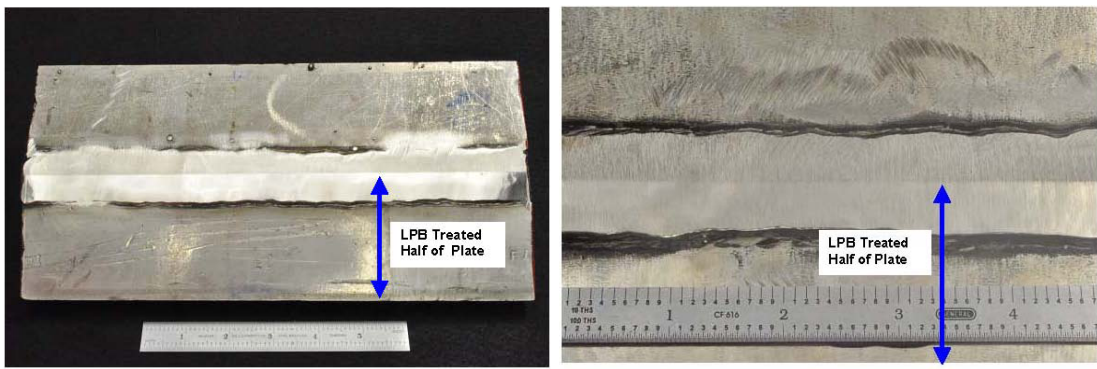


Figure 2: 304L SS Half LPB processed plate specimen.

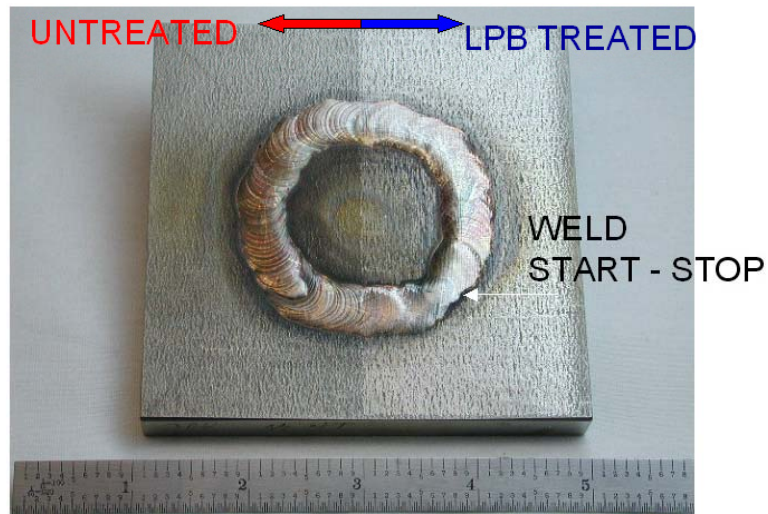


Figure 3: Half LPB processed 316L Plate Specimen

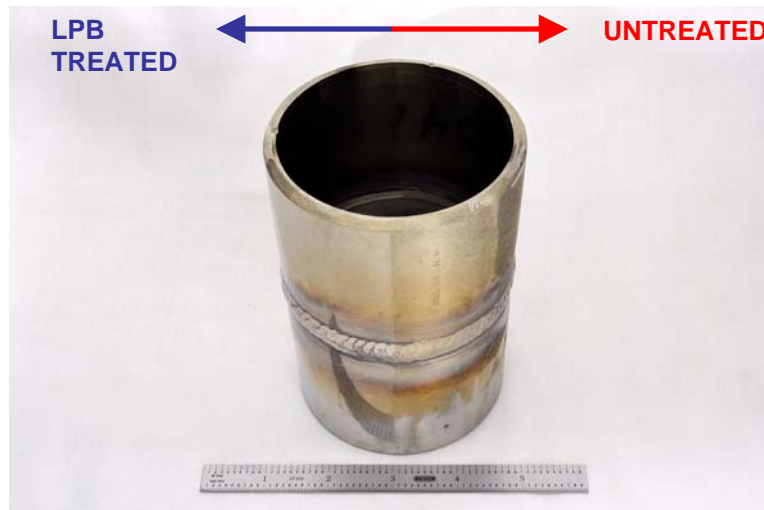


Figure 4: 304L SS circular weld plate specimen. 1/2 LPB Processed 316LSS welded pipe specimen; half LPB processed on inside and outside diameter.

### Residual Stress Field Characterization

X-ray diffraction residual stress and cold work measurements were made on the specimens to characterize the effect from welding and LPB processing as both a function of depth and as a function of distance across the welds and HAZ. X-ray diffraction measurements were performed using a  $\text{Sin}^2\psi$  method, in accordance with SAE J784a.<sup>13</sup> X-ray diffraction residual stress measurements were made at the surface and at several depths below the surface on the specimens. Material was removed electrolytically for subsurface measurement in order to minimize possible alteration of the subsurface residual stress distribution as a result of material removal. The residual stress measurements were corrected for both the penetration of the radiation into the subsurface stress gradient<sup>13</sup> and for stress relaxation caused by layer removal.<sup>14-17</sup>

### SCC Testing

SCC test specimens were subjected to up to 100 hours constant immersion in hot/boiling  $\text{MgCl}_2$  above  $120^\circ\text{C}$ . Specimens were removed from solution and observed following exposure. Optical microscopy and fluorescent dye penetrant were used to inspect for, and reveal SCC on the specimens.

### Mechanical Stability Testing

Separate test specimens were specifically machined in order to characterize the mechanical stability of the LPB induced compressive residual stress. Test samples with dimensions of 0.625 x 1.25 x 12 in. (15.9 x 31.8 x 304.8 mm) were manufactured from 304L and 316L SS. The test specimens were LPB processed on the active faces. Following LPB treatment the specimens were instrumented with strain gage rosettes to monitor the strains applied via 3-point bending. A picture of a sample mounted in the 3-point bend fixture on the hydraulic test frame is shown in Figure 5.

A wide range of tensile strains was applied over the length of the sample including strains well beyond the proportional limit of the materials tested. Residual stresses were mapped on the mechanically cycled 3-point bend specimens. Measurements were made in the longitudinal direction as a function of distance from the center of the bend.

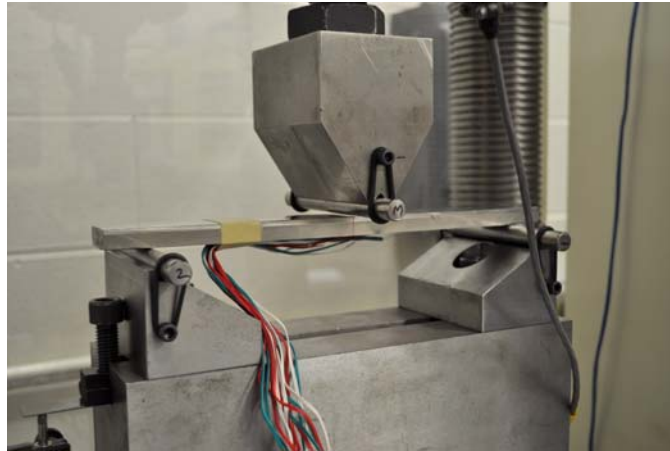


**Figure 5: Mechanical stability 3-pt bend test sample mounted in loading fixture on a hydraulic loading frame.**

### **Thermal Stability Testing**

One 304L and one 316L LPB processed test specimen was exposed to 650°F (343°C) for 100 hrs. A temperature of 650°F (343°C) was chosen because it is the upper end of the operating temperature of a reactor system. X-ray diffraction residual stress measurements were made on a baseline sample and a thermally exposed sample in order to determine the thermal stability of the residual compression from LPB.

### **Surface Roughness**

Surface roughness measurements were performed on both the untreated and LPB treated sides of the plate specimens respectively using a Mitutoyo SJ-201 surface roughness tester. The Ra surface roughness was calculated over a 0.50 in. evaluation length parallel and perpendicular to the longitudinal axis of the plate.

## **EXPERIMENTAL RESULTS**

### **Residual Stress Characterization**

Welded plates of each material and geometry were processed identically; one plate from each group was used for XRD residual stress analysis and the remainder for SCC testing. There is likely some variation between the location of the SCC cracks and the location of the high-tension region adjacent to the weld between the plates used for SCC testing and the plate used for X-ray stress analysis. The compressive residual stresses produced by LPB prevented SCC from initiating in all cases.

Figure 5 shows the residual stress distribution as a function of distance and depth for a 304L circular welded plate in both the LPB treated and un-treated regions. Tensile residual stresses on the as-welded side of the sample approach +100 ksi (+689 MPa). The LPB treatment produced deep compression with a magnitude of greater than -120 ksi (-827 MPa). Figure 6 shows the residual stress distribution as a function of distance and depth for a 316L welded rectangular plate in both the LPB treated and un-treated regions. Tensile residual stresses on the as-welded side of the sample exceed +100 ksi (+689 MPa). The LPB treatment produced deep compression with a magnitude of greater than -90 ksi (-620 MPa).

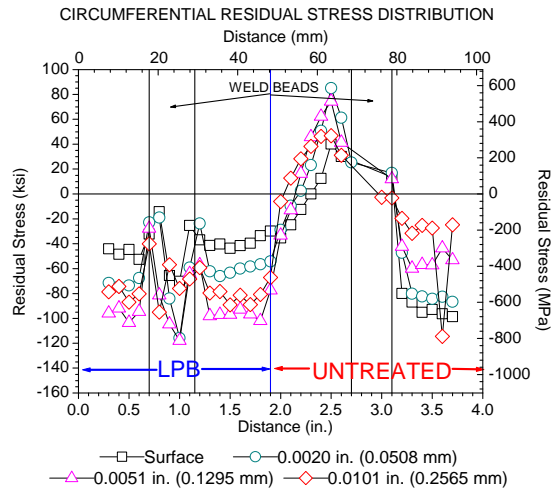


Figure 6: XRD residual stress measurements on half LPB treated welded 304L SS plate. The LPB processed region is in deep compression across the weld while the untreated half is in high tension.

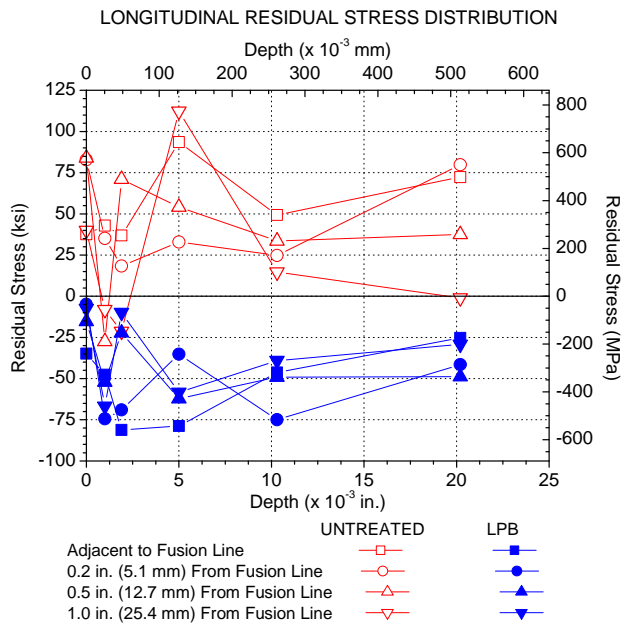


Figure 7: Longitudinal residual stress vs. depth on a 316L welded plate. The LPB processed half remains in a compressive state out past 1.0 in from the fusion line. High magnitude tensile stress is present on the untreated half of the plate.

## SCC Testing Results

The untreated half of all tested specimens suffered severe through thickness SCC damage. The LPB processed half of all tested specimens showed no evidence of SCC for all geometries tested. All tested specimens were examined via optical microscopy at up to 60X magnification and a fluorescent dye penetrant was used to reveal SCC. Cracking on the un-processed sides of the welds and base material was characteristic of SCC with cracks running near perpendicular to the directions of maximum residual tensile stresses. The majority of cracking was observed in the region 0.15 in. to 1.25 in. (3.8 to 31.8 mm) from the fusion line of the weld.

Photographs shown in Figure 7 show a 304L and 316L SS circular weld specimen after 100 hours exposure to hot/boiling  $MgCl_2$  above 120° C. The extent of the damage on the untreated half of the specimens is obvious. Cracking is observed in both the hoop and radial directions and is a direct result of the tensile stress field on the untreated material; the cracking terminates precisely at the boundary of the LPB processing. Figure 8 shows a cross section of a 304L specimen revealing through thickness cracking on the untreated material. Figures 9 – 13 show the SCC damage sustained by the rectangular welded specimens after 100-hour exposure in  $MgCl_2$ . Again the untreated material suffered severe SCC damage. Areas of grinder burn were also initiation points for SCC on the unprocessed half of the specimen. LPB prevented this on the processed halves which also had grinder burns. Cross sectional examination of the specimens reveal the depth of the cracking extends approximately 0.5 in and terminates near the toe of the weld.

Figure 14 shows a 304L pipe weld specimen after 24 hours of  $MgCl_2$  exposure. The untreated material again exhibited severe through thickness SCC cracking. Examination of all tested samples revealed no evidence of SCC on the compressive LPB processed side. The un-processed side of all specimens tested developed extensive SCC.

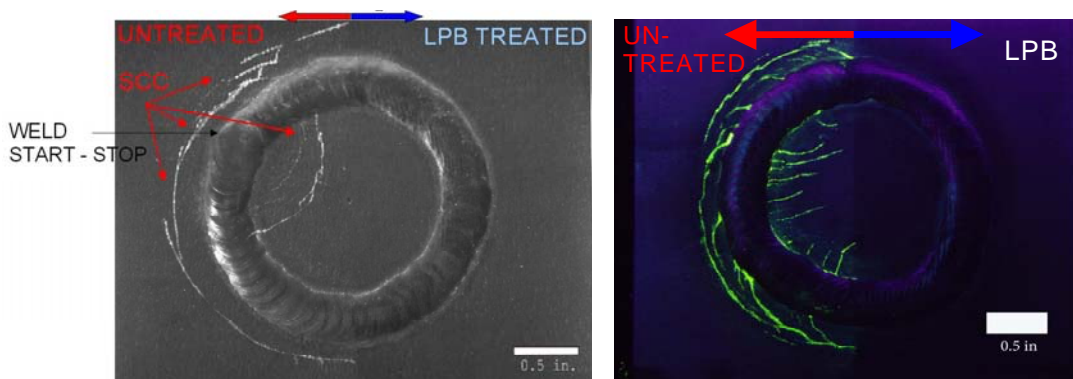


**Figure 8: Black light fluorescent dye defines severe SCC on un-treated side of 304L (left photo) and 316L SS circular weld (right photo) specimens.**

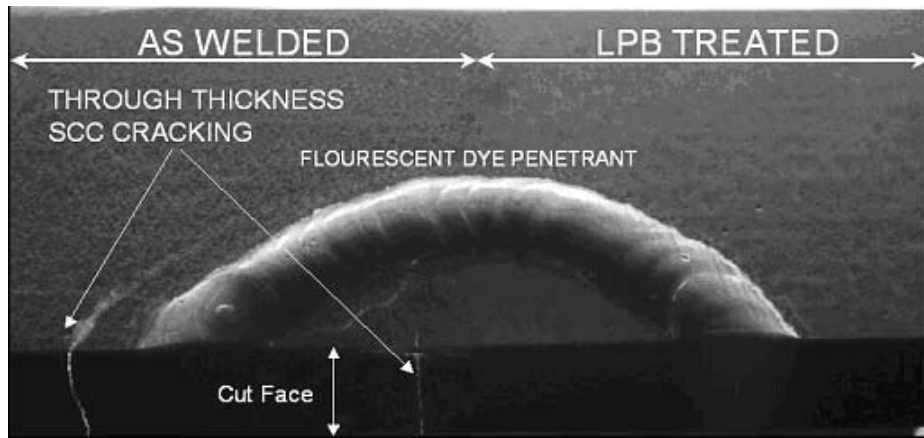


Figure 9: Fluorescent dye penetrant photo showing through thickness SCC cracking on untreated side of 304L SS circular weld specimen.

## POST SCC TESTING - 304

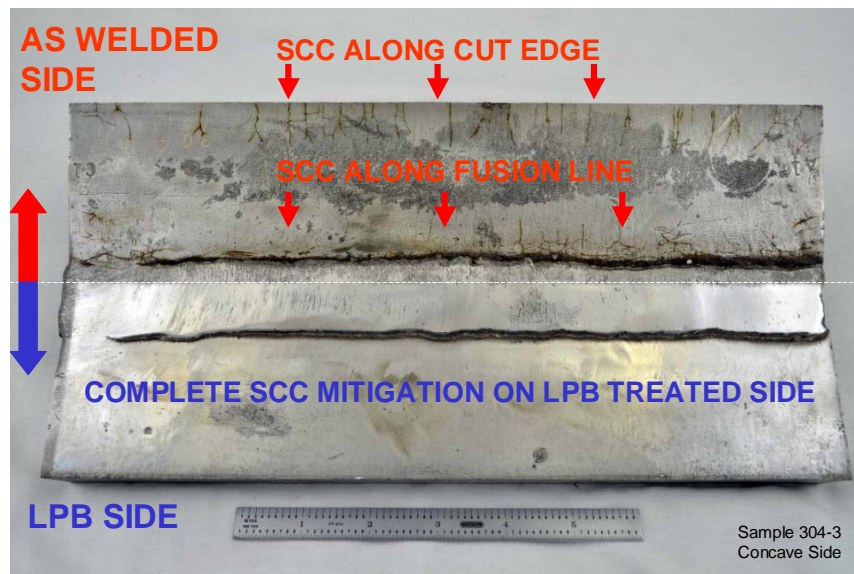


Figure 10: Sample 304-3 following  $MgCl_2$  exposure showing severe SCC on untreated concave side and no SCC on LPB treated side of plate.

# POST SCC TESTING - 304

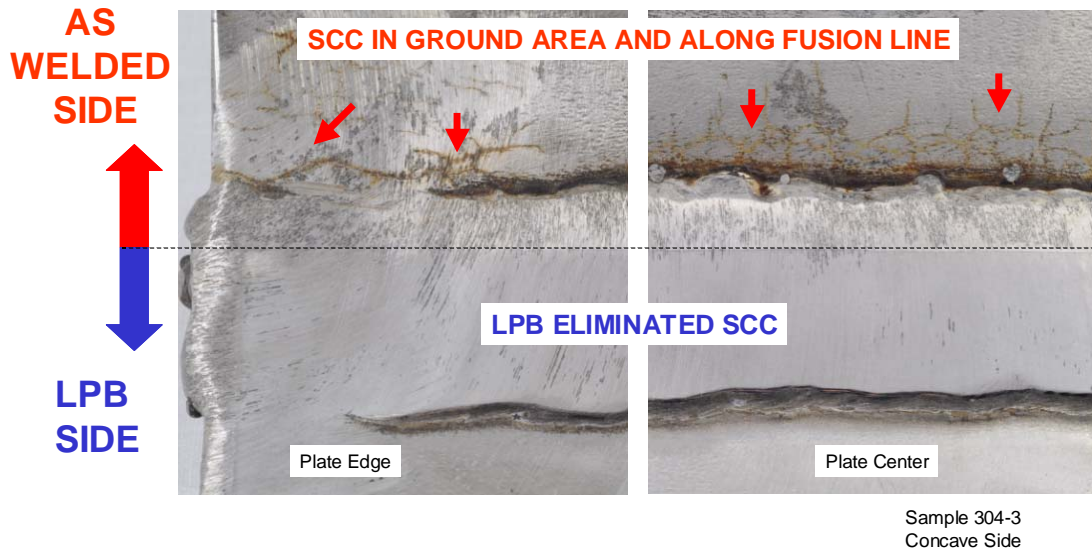


Figure 11: Close-up of Sample 304-3 fusion line on concave side following  $MgCl_2$  exposure showing extensive SCC in ground region and along fusion line on untreated region.

# POST SCC TESTING - 304

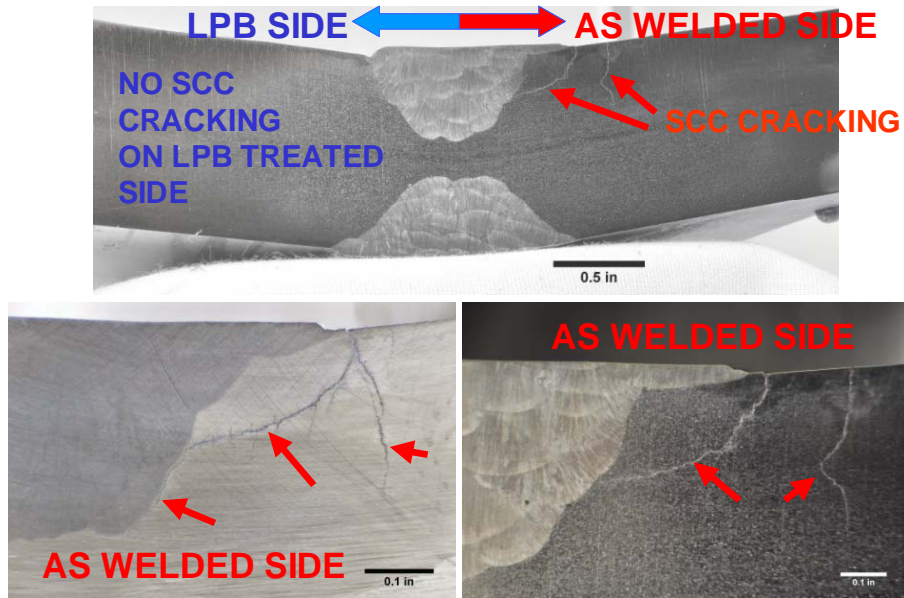


Figure 12: Cross section of Sample 304-3 showing deep SCC in heat affected zone on untreated side of test plate and no SCC on LPB treated side of plate.

# POST SCC TESTING - 316



Figure 13: Close-up of Sample 316-3 fusion line on convex side following  $MgCl_2$  exposure revealing SCC along fusion line and in ground regions on untreated side and no SCC on LPB side.

# POST SCC TESTING - 316

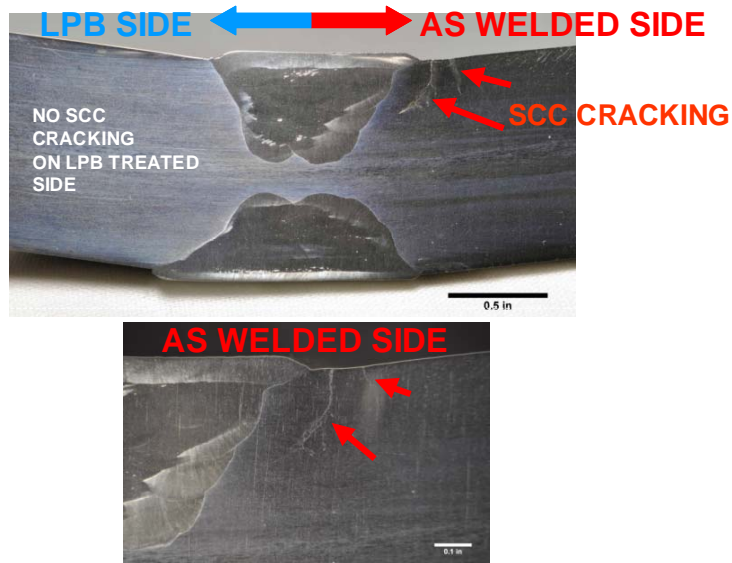


Figure 14: Cross section of Sample 316-3 showing deep SCC in heat affected zone on untreated side of test plate and no SCC on LPB treated side of plate.

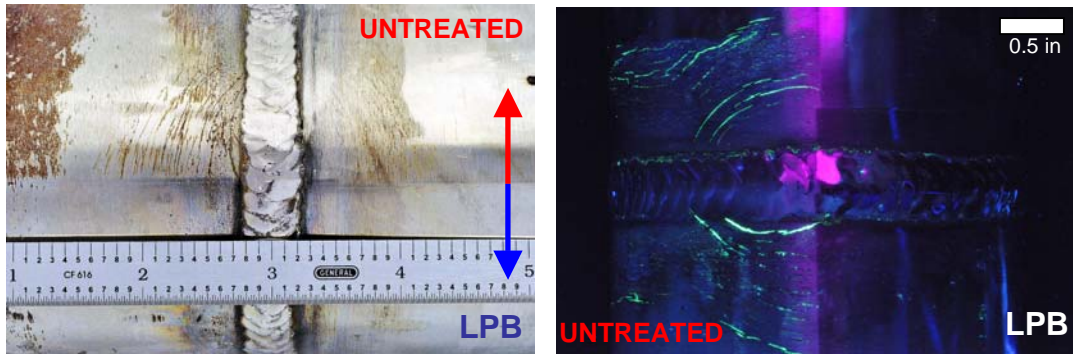


Figure 15: SCC cracking on un-treated side of a 304L SS pipe weld specimen. The photo on the right is a fluorescent dye image of the same specimen shown on left. No cracking was found on the LPB processed regions any specimens.

### Mechanical Stability Results

Figures 16 and 17 show the resulting residual stress distributions for each alloy after mechanical stability testing. The compression from LPB shows only a small reduction in magnitude even at applied strains well above the proportional limit of the material. During the initial reactor start-up cycle dissimilar butt weld joints may experience total strains as high as 0.6%, which is well into the plastic regime for the alloys studied.

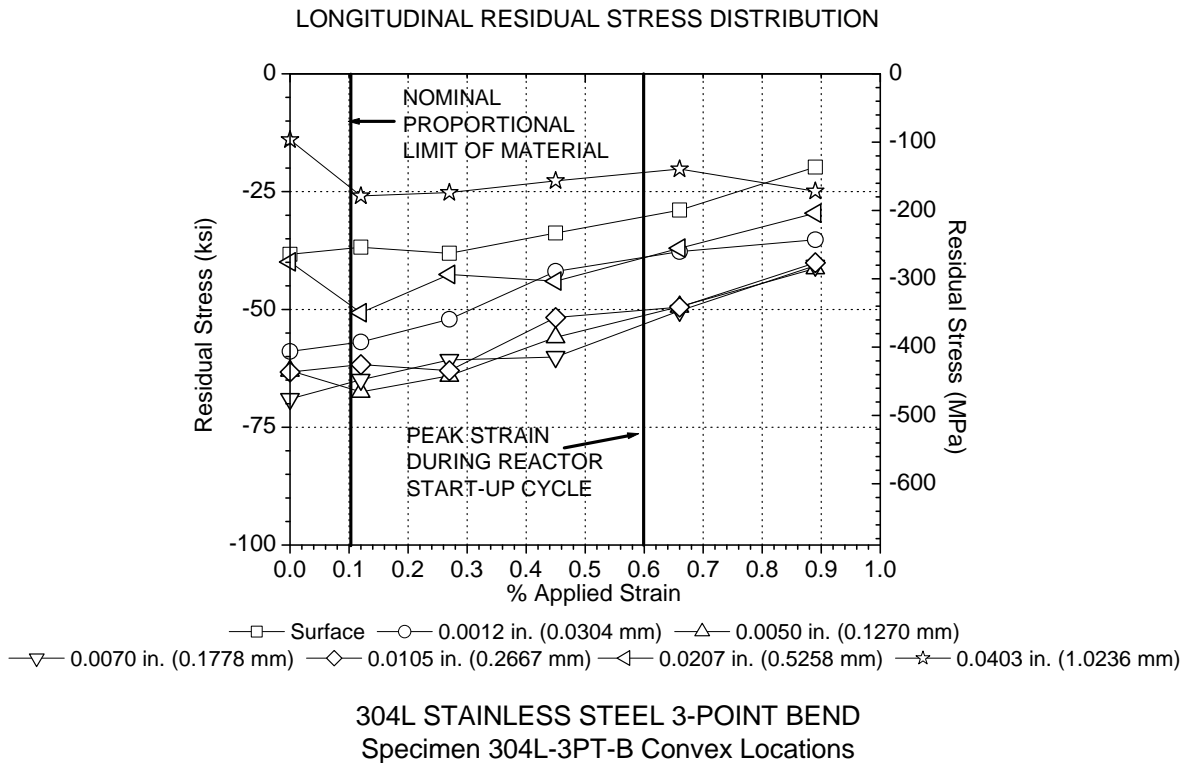
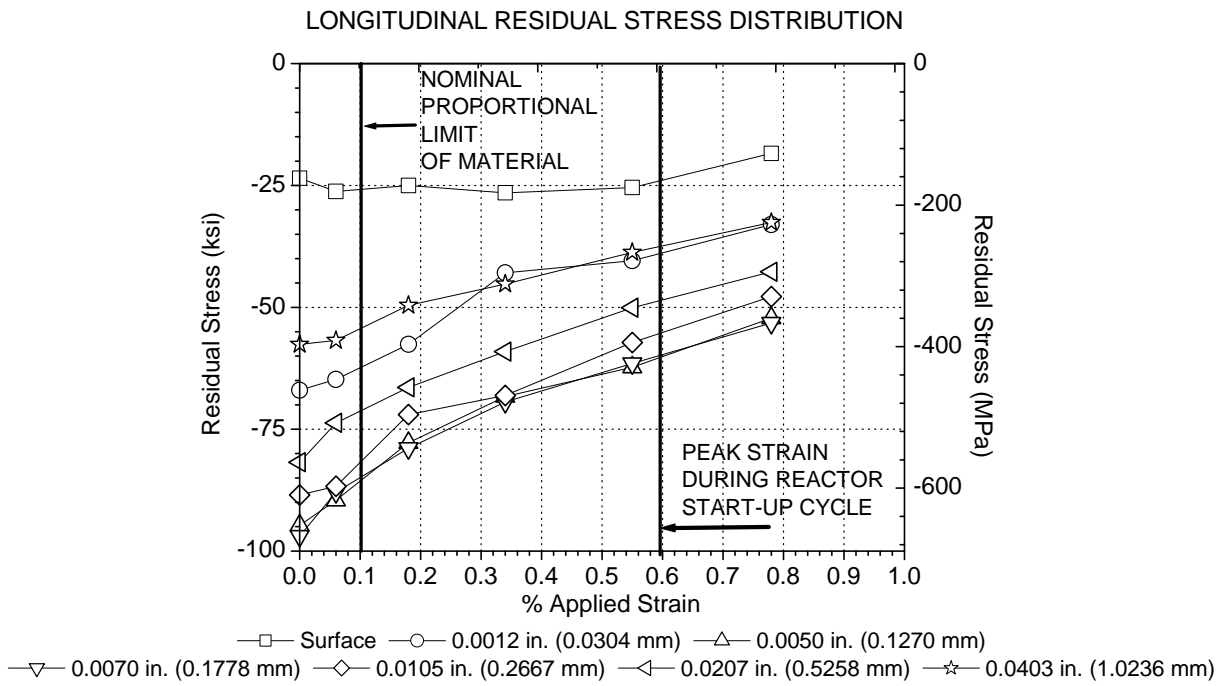


Figure 16: Longitudinal residual stress on 304L 3 point bend sample.

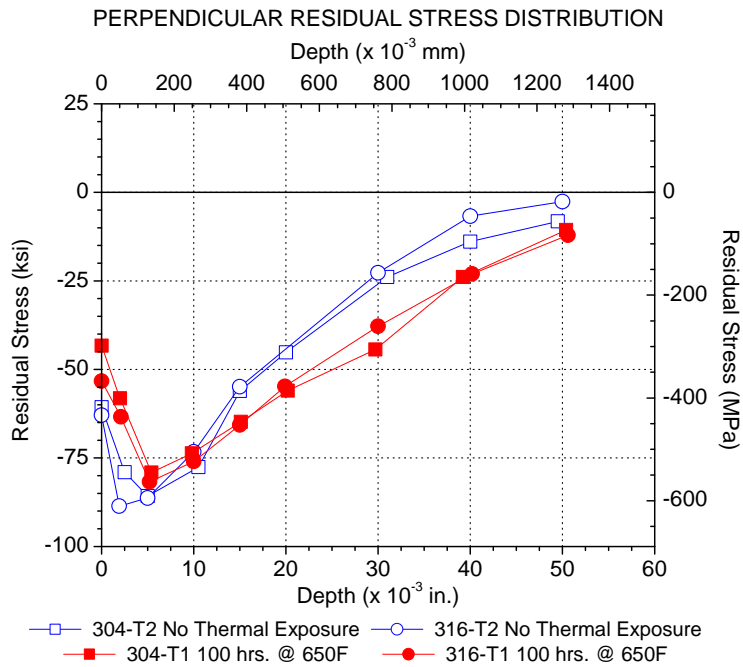


316L STAINLESS STEEL 3-POINT BEND  
Specimen 316-3PT-B Convex Locations

**Figure 17:— Longitudinal residual stress on 316L 3-point bend sample.**

### Thermal Stability Results

Figure 18 shows the residual stresses as a function of depth. Depth of compression resulting from LPB is on the order of 0.05 in. Results indicate only a slight reduction in near surface compression as a result of the thermal exposure.



STAINLESS STEEL LPB PROCESSED PLATES  
Center of LPB Processed Region

**Figure 18: Residual stress vs. depth for both thermally treated specimens and unexposed baseline specimens.**

**Surface Roughness Results**

Surface roughness results are presented graphically in Figure 15. The LPB treatment dramatically improved the surface finish. Surface roughness in the parallel and perpendicular direction was reduced on average by nominally 95% due to LPB. The smoother surface finish produced by LPB is understood to be beneficial in non-destructive examination.

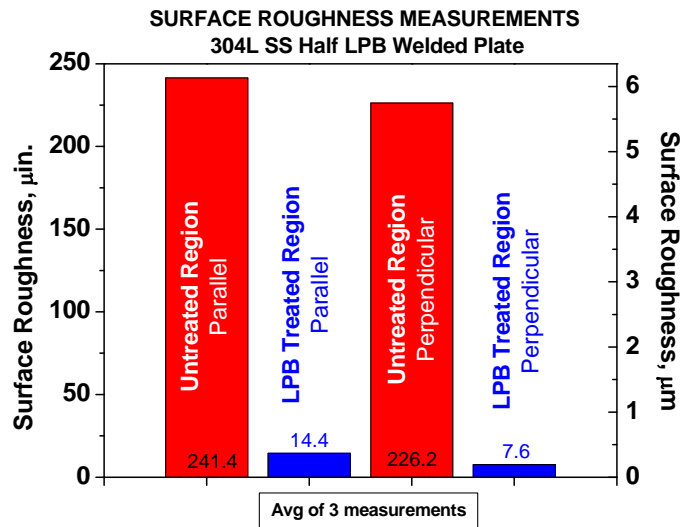


Figure 19: Average Ra surface roughness of specimen on un-treated and LPB treated regions. LPB produced a greatly improved surface finish with an average improvement of 95% Ra.

## CONCLUSIONS

- The use of compressive residual stress on 304L and 316L SS is a viable method of preventing/mitigating SCC.
- Welding produces high tensile residual stresses of greater than +100 ksi (+689 MPa) at the surface and into the near surface material of both 304L and 316L SS.
- Compression from LPB is stable after thermal exposure and mechanical cycling even beyond the proportional limits of the materials.
- LPB processing provides greater depth of compression than conventional shot peening protecting surfaces against SCC with the added benefit of low of cold working for thermally stable residual compression.
- SCC testing of LPB treated 304L and 316L SS weldments showed a complete mitigation of SCC.
- LPB processing improved the surface finish of treated specimens by 95% on average.

## REFERENCES

1. P.L. Andresson and M.M. Morra, "SCC of Stainless Steels and Ni Alloys in High-Temperature Water" Journal of science and Engineering Corrosion., Vol. 64, No. 1. pg. 15., 2008.
2. "Primary system Corrosion Research." EPRI Portfolio 2008. EPRI Website 11/12/07 <http://portfolio.epri.com/project.aspx>
3. D.H. Hornbach and P.S. Prevey, "Tensile Residual Stress Fields Produced in Austenitic Alloy Weldments," Proceedings: Energy Week Conference Book IV, Jan. 28-30, Houston, TX, ASME International, 1997.
4. .P.S. Prevey, et al. "Effect of Prior Machining Deformation on the Development of Tensile residual Stresses in Weld Fabricated Nuclear Components" Journal of Materials Engineering and Performance, vol. 5(1), Materials Park, OH; ASM International, 1996 pp. 51-56.
5. Fontana, Mars G. Corrosion Engineering. McGraw-Hill, Inc., 1986
6. P.S. Prevey., "X-RAY Diffraction Characterization of Residual Stresses Produced by Shot Peening" Shot Peening Theory and Application, series ed. A. Niku-Lari, IITT-International, Gournay-Sur-Marne, France, 1990, pp. 81-93.
7. O. Oyamada, et. Al., "Prevention of Stress Corrosion Cracking by Water Jet Peening: , Proc. 5<sup>th</sup> Int. Conf. Nuclear Eng. ASME (1997).
8. M. Yoda et. Al., "Development and Application of Laser Peening System for PWR Power Plants" ICONE14, July 17-20, Miami, Fl. ICONE14-89228.
9. N. Jayaraman and P. Prevey., "Comparison of Mechanical Suppression by Shot Peening and LPB to Mitigate SCC and Corrosion Fatigue Failures in 300M landing Gear Steel." Proceedings of ICSP 9 (Paper 259) Paris, Marne la Vallee, France, Sept. 6-9, 2005.
10. P.S. Prevey et. Al., "Mechanical Suppression of SCC and Corrosion Fatigue Failures in 300M Steel Landing Gear" Proceedings of ASIP 2004., Nov. 29-Dec. 2, 2004, Memphis, TN.
11. P.S. Prevey, "The Effect of Cold Work on the Thermal Stability of Residual Compression in Surface Enhanced In 718" Proceedings: 20<sup>th</sup> ASM Materials Solutions Conference & Exposition, St. Louis, MO, Oct 10-12,2000.
12. N. Jayaraman and P.S. Prevey. "A Design Methodology to take credit for Residual Stresses in Fatigue Limited Designs" Journal of ASTM International, Vol. 2, issue 8 Sept. 2005.
13. P.S. Prevey. "X-RAY Diffraction Residual Stress Techniques" Metals Handbook, 10, Metals Park, OH: ASM, 1986, pp.380.
14. Moore, M.G. and Evans, W.P., (1958) "Mathematical Correction for Stress in Removed Layers in X-Ray Diffraction Residual Stress Analysis," SAE Transactions, 66, pp. 340-345.
15. Hilley, M.E. ed.,(2003), Residual Stress Measurement by X-Ray Diffraction, HSJ784, (Warrendale, PA: SAE).
16. [Noyan, I.C. and Cohen, J.B., (1987) Residual Stress Measurement by Diffraction and Interpretation, (New York, NY: Springer-Verlag).
17. Cullity, B.D., (1978) Elements of X-ray Diffraction, 2nd ed., (Reading, MA: Addison-Wesley), pp. 447-476